

Annealing and melting of long-chain alkane single crystals observed by atomic force microscopy

A.K. Winkel*, J.K. Hobbs, M.J. Miles

H.H. Wills Physics Laboratory, Royal Fort, Tyndall Avenue, Bristol BS8 1TL, UK

Received 4 October 1999; received in revised form 13 January 2000; accepted 25 January 2000

Abstract

The annealing behaviour of once-folded crystals of the long-chain alkane, $C_{162}H_{326}$, is examined in situ, in real time, by atomic force microscopy. Regions of thickening material can be clearly seen in the height images. The formation of dendritic patterns is observed and holes are often formed at the growth front. These holes do not form after comparable treatment of initially extended chain crystals of the same material. The heating of the extended chain crystals shows a highly mobile phase just before melting. The fact that no holes or dendritic patterns emerge before the melting of the extended chain crystal leads us to attribute this phenomenon to the thickening process. The holes are formed at the growth front as a means of relieving the strain. The formation of the dendritic structures is also a result of strain: as the strain builds up in the current growth direction, so the growth changes to an alternate crystallographic direction. © 2000 Elsevier Science Ltd. All rights reserved.

Keywords: Thickening process; *n*-Alkanes; Polymers

1. Introduction

This work is part of an on-going project in our laboratory utilising strictly monodisperse, ultra-long *n*-alkanes [1–4], recently available in gram quantities from G. Brooke [5] and the Engineering and Physical Sciences Research Council of the UK (EPSRC). These materials provide an ideal model system for polyethylene, having lengths sufficiently long to display chain folding but, being strictly monodisperse, are free from many of the complications inherent to high polymers. Previous studies have already provided a wealth of information and new insights into the crystallisation and melting behaviour of polymers [6–10]. Of particular importance in the present context are observations relating to integer-folding [6], transient non-integer states [7,8,11], and crystal thickening [9,10].

The work to be reported here is part of a preliminary study, using atomic force microscopy (AFM), of the solid-state lamellar thickening process that these materials, in common with polyethylene [12] and many other polymers e.g. [13], undergo on annealing at elevated temperatures. Here we are dealing with the thickening of single crystals, grown in dilute solution, that have subsequently been dried

down onto a substrate and annealed at elevated temperatures. This is in contrast to another paper by one of us which deals with isothermal thickening of solution-grown alkane crystals [4] still suspended in solution.

Lamellar thickening has been extensively studied in many polymer systems as it is an industrially important process, as well as being of considerable interest from a scientific viewpoint as it gives an indication of both the driving force towards the equilibrium (extended chain) crystal conformation, and of the barriers to molecular motion. In melt crystallised polymers and dried single crystal mats, the thickening process has primarily been followed both in situ and ex situ by X-ray scattering see e.g. [13–15] and, to a lesser extent, by Raman LAM [15,16], and ex situ by TEM of sectioned, stained or etched samples. The high temperature annealing of solution-grown single crystals has been studied in a variety of polymers using TEM, usually by drying the crystals down onto a substrate before heating, although some experiments have been performed on single crystal suspensions in silicon oil. For extensive reviews on earlier work in this field see Wunderlich [13] and Geil [14]. More recent work has extended the X-ray studies by use of synchrotron radiation to allow real-time monitoring of changes in thickness over time-scales of seconds [16], and the study of single crystals has been extended to include polyethylene single crystals crystallised at high temperatures and possessing curved crystal surfaces [17].

* Corresponding author. Fax: +44-117-925-5624.

E-mail address: alex.winkel@bristol.ac.uk (A.K. Winkel).

In most cases thickening has been found to be a gradual process, both the thickening rate and the final thickness attained increasing with increasing annealing temperature [13]. In some exceptional cases integer doubling of crystal thickness has been observed, particularly in single crystal mats [16], and it has been postulated that this minimises the necessity for co-operative molecular motion [18]. In the case of thickening of bulk samples, voiding is relatively rare, as volume is approximately conserved (assuming crystallinity remains constant) and the bulk surface area is small compared to its volume. However, the situation in dried down single crystal lamellae is clearly very different, as all of the thickened material must come from the surrounding single layer. This generally leads to voiding and a complex thickened morphology of holes separating thickened arms and islands of material within the perimeter of the original, unthickened, crystal [14], sometimes described as a “Swiss cheese” morphology.

In high polymers the thickening process is further complicated by the polydispersity which is present in even the sharpest fractions available. Crystal stability, and therefore the rate of thickening, will clearly depend not only on the average chain length, but also on the range of chain lengths in the sample, any fractionation that may have occurred during the initial crystallisation process, and on the level of chemical perfection (e.g. branching and tacticity). Many of these problems can be avoided by the use of the ultra-long chain, strictly monodisperse alkanes, which are the subject of the present study.

In the work reported here we have used AFM to follow the re-organisation that occurs on high temperature annealing. AFM is a relatively young technique [19], with an ever-growing number of applications. The technique involves bringing a very sharp probe on the end of a cantilever close to the surface and using feedback to maintain the level of the interaction with the surface. In the study reported here, Tapping Mode is used, which involves oscillating the tip in the direction normal to the plane of the sample and maintaining the amplitude of this oscillation at some pre-set value, as the tip taps the surface and scans over the topography of the specimen.

Over recent years there have been an increasing number of studies using AFM to follow processes in polymers in real time. AFM is a fairly non-destructive technique, that allows direct observation of the surface of the sample without the staining or metal coating required by electron microscopy, and unlike scanning tunnelling microscopy (STM) [20], does not depend on the sample being electrically conducting. Examples of these applications include polymerisation, crystallisation, melting and degradation. In 1989 Drake et al. [21] outlined some of the potential of the AFM, including the fact that it is possible to study polymer surfaces and processes. A number of studies have been made of in situ spherulitic crystallisation and melting in a variety of polymers, and provided significant and surprising new insights into the kinetics of this ubiquitous form of

crystal growth [22–27]. It has also been possible to follow degradation processes in situ, including the degradation of a spun cast thin film of a poly(ortho ester) in a hydrolysing environment [28], PHB being degraded by different types of extracellular depolymerases [29] and starch being enzymatically degraded [30].

Although high temperature annealing has been extensively studied, it has not previously been possible to follow the thickening process in real time on a microscopic scale, without the averaging inherent in scattering techniques, due to the beam damage caused by electron microscopy. The work presented here is the first study of in situ crystal thickening in a polymer system, using AFM coupled with a heating stage, allowing us to image the development of the thickened morphology and access directly the kinetics of the process on a sub-micron scale. By utilising the strictly monodisperse alkanes which undergo integer folding (in the present case of $C_{162}H_{326}$, strictly integer once-folded (1F) and extended chain crystals can be crystallised in dilute solution) the thickening process can be considerably simplified with respect to that found in high polymers. However, we recognise that the chains are considerably shorter than those commonly found in commercial polymers, increasing considerably the freedom for molecular motion. Thus some of the types of behaviour that we have observed here may be confined to shorter molecules in which the level of chain entanglement is low, and the degree of crystallinity is high. A second caveat is that the present study deals only with single crystals dried onto a mica substrate, adding an additional level of constraint that is not commonly present when annealing polymers. The potential of AFM to improve our understanding of the thickening processes, is, however, clear from the preliminary work presented below.

2. Experimental details

G. Brooke [5] and the EPSRC kindly provided the materials used in this study.

Samples of $C_{162}H_{326}$ were weighed into glass tubes and toluene added to give a concentration of $\sim 0.01\%$ (w/v). The glass tubes were then flame sealed to prevent the volatile solvent from escaping during crystallisation, and placed into a pre-heated oil bath at 105°C for 5 min. The sample was quenched and inspected to ensure that a cloudy suspension had formed, indicating that all the parent material had dissolved. The suspension was then redissolved, once more at 105°C for 5 min, and moved to a pre-heated oil bath at the selected crystallisation temperature. Crystallisation at 60°C for 30 min followed by slow cooling resulted in once-folded single crystals of $C_{162}H_{326}$ free from the surface decoration that occurs on quenching. Crystallising at 70°C for 48 h and cooling slowly resulted in extended chain single crystals. In this latter preparation there were also occasional once-folded crystals that had crystallised during

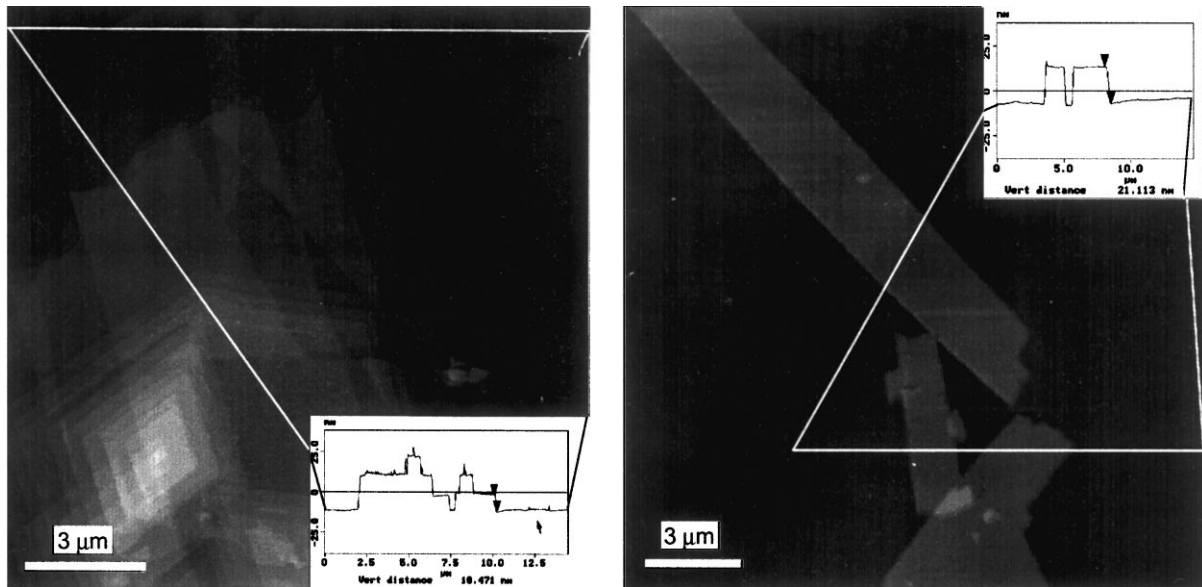


Fig. 1. The lower resolution height images of $C_{16}H_{32}$ crystals. The left-hand image is of an aggregation of once-folded (1F) single crystals. The inset shows a cross-section analysis indicating that the thickness, about 11 nm, is close to the expected value of 10.4 nm. The right-hand image shows extended chain (E) single crystals. A section analysis is presented in the inset showing that the thickness, 21 nm, is close to the expected value (20.8 nm).

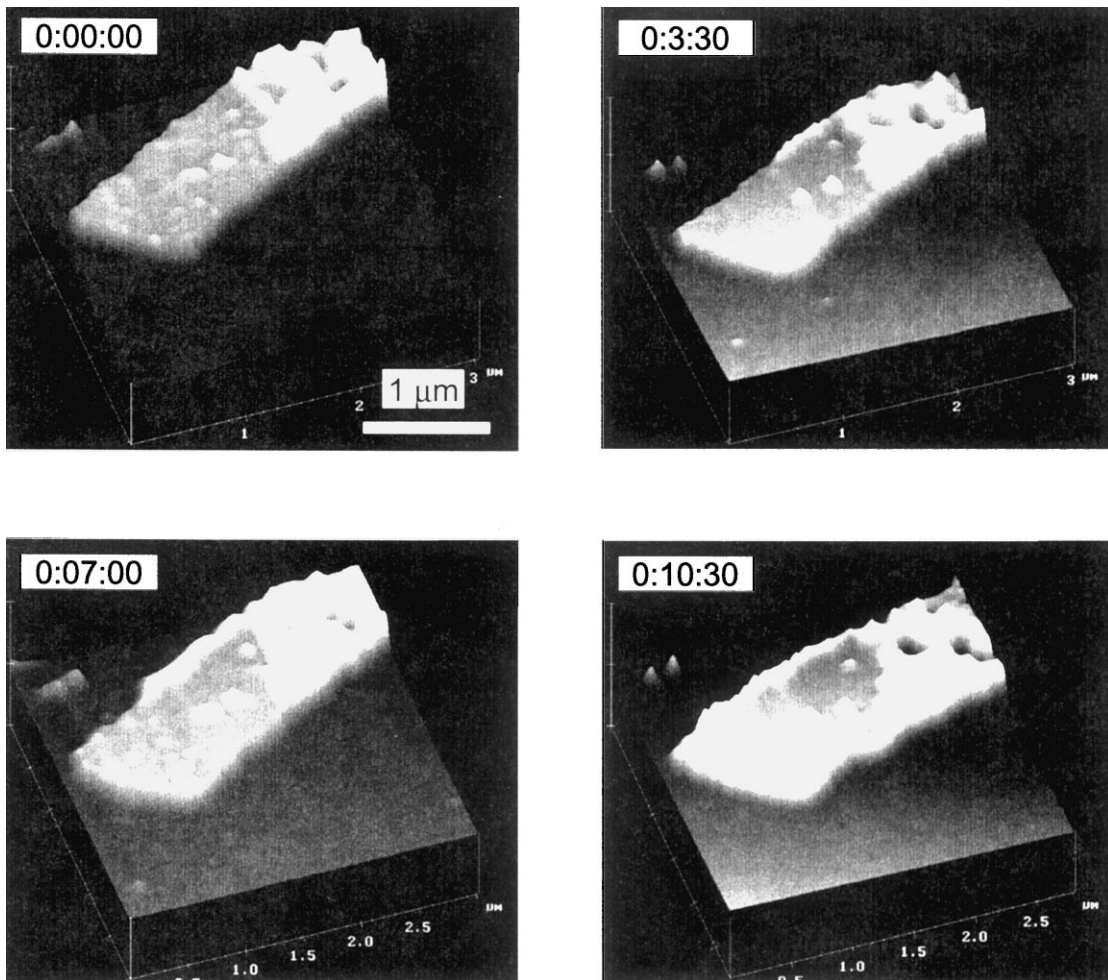


Fig. 2. A sequence of four height images obtained during thickening of once-folded $C_{16}H_{32}$. The temperature was a nominal $100^{\circ}C$. The extended phase propagates quickly along the edges of the crystal.

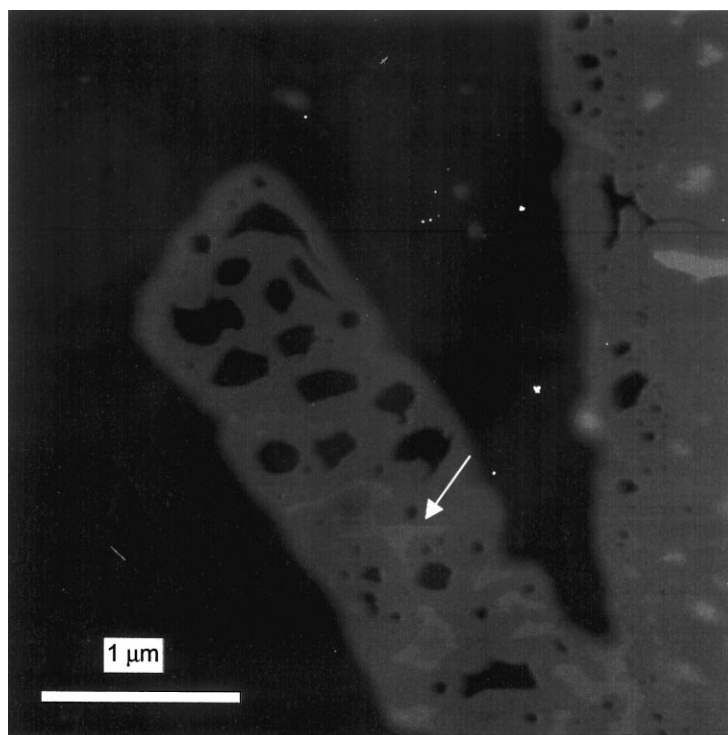


Fig. 3. A height image, taken at room temperature, of the same crystal as in Fig. 2, shows the holes that formed during the thickening experiment. The image size is $3.7 \times 3.7 \mu\text{m}^2$. The arrow indicates a small region of material which is thicker than the rest of the crystal.

cooling (unfortunately hot filtering was not possible owing to the very limited amount of material available).

The dilute crystalline suspensions were then pipetted onto freshly cleaved mica, which was glued to a stainless steel sample disc. These samples were imaged using a Digital Instruments D3100 AFM, operated in Tapping Mode, using the standard silicon probes. The heater used was a heating and freezing stage produced by Linkam Scientific Instruments. In the first experiment this heater was used in conjunction with a non-standard sample stub. The disadvantage of using this approach was that the temperature readings displayed do not represent the sample temperature very closely since there will be both a thermal gradient as well as a thermal lag across the thicker stub.

For further experiments, a modification was made to the apparatus to allow the use of thinner sample stubs. Another addition was an aluminium heat shield designed to protect the thermally sensitive piezo material in the AFM scan tube from damage. The protection was further increased for the higher temperatures with a gentle nitrogen flow over the top of the heat shield. A small hole was cut in the aluminium shield to allow the AFM tip to access the surface.

The Linkam controller is capable of low heating rates, which are essential if a heating process is to be followed in situ by AFM, otherwise the thermal expansion would be too fast. Generally, heating rates in the range $0.1\text{--}0.5^\circ\text{C}/\text{min}$ were chosen. Another important consideration is the Linkam's ability to maintain its set temperature very precisely (in the order of a tenth of a degree).

3. Results

Fig. 1 shows a pair of AFM images of typical single crystal morphologies for the $\text{C}_{162}\text{H}_{326}$ crystals, which are the primary subject of this study. Many of the crystals are rectangular 110 twins, which are attached to very large aggregates. The high level of aggregation occurs because, in these high purity monodisperse systems, it is very difficult to use self-seeding techniques, so the nucleation density is very low. In a number of the rectangular twins pleats are visible parallel to 110 planes, presumably formed during the collapse of the crystal onto the substrate. The inset on Fig. 1a shows a cross-section taken of one of the crystals, from which the crystal thickness of 11 nm can be measured, which is reasonably close to the expected value of 10.4 nm for a chain folded exactly in half (allowing no carbons for the fold, so we might expect the true thickness to be slightly thinner than this). Similar cross-sections taken of extended chain crystals give a thickness of 21 nm, in good agreement with the expected thickness of 20.8 nm for perpendicular chains. The reason for the slightly larger than expected thickness of the 1F material is unclear, although we may speculate that either some disorder on the crystal surface, or lack of planarity perhaps caused by the process of collapse onto the substrate, may cause an increase in thickness. These thicknesses agree not only with expected values (based on chain lengths), but also with experimental values as measured by both Raman LAM and X-ray studies (unpublished data).

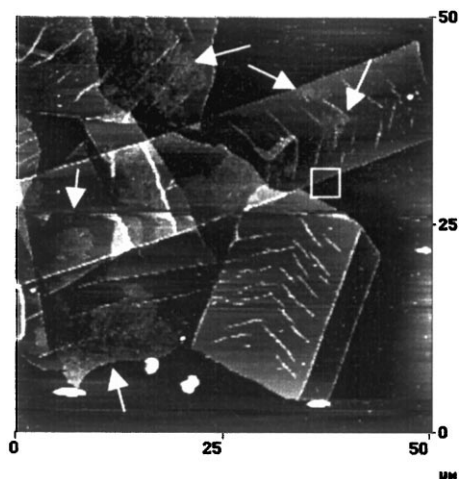


Fig. 4. A low resolution height image of the surrounding morphology of the crystals in the 90°C isothermal annealing experiment, taken after approximately 2 h of annealing. Some areas can be seen to have already thickened (as indicated by the arrows). The box indicates the approximate area examined at higher resolution later and shown in Figs. 5–7.

Fig. 2 shows a series of “3D” representations of AFM images taken consecutively during the heating of a 1F sample at 1°/min at ~100°C (the sample itself was at a somewhat lower temperature than this owing to the temperature lag at these rates of heating and the relatively thick sample stub used in this experiment). The particular crystal in this sequence was a small fragment and the precise crystallography is unclear. The brighter regions in the images are the thickened material. A thickening front can be seen progressing leftward from the part of the crystal to the right of the image. A striking feature here is the preferential thickening along the top edge of the crystal, from which a propagation rate of 2.5 ± 0.5 nm/s can be measured. The height of the thickened region is 17–20 nm which is consistent with extended chain crystals, perhaps in some regions tilted at an angle of 35° to the lamellar normal. This angle of tilt is commonly found both on melt crystallisation and on high temperature annealing of solution grown mats of the long alkanes. After thickening had occurred the crystal was annealed for 70 min at ~110°C and cooled during the next 80 min to ~84°C, finally cooling to ~37°C during a further 20 min. At ~110°C the thickness of the crystal was in the range 16–17.5 nm, consistent with tilted chains. Fig. 3 shows the crystal after cooling. This crystal closely resembles the “Swiss cheese” type morphologies found on annealing polyethylene single crystals on a substrate. Two features are of particular interest. Firstly the crystal is 20.5–21 nm thick, that is, it consists of extended chains perpendicular to the substrate, so the chains must have passed through a process of “un-tilting”. Secondly, there are a number of regions approximately 1 nm higher than the rest of the crystal (an example is arrowed). It is possible that this is a layer of contamination (perhaps $C_{162}H_{326}$ chains lying in the plane of the crystal surface). Alternatively it may be that there are domains within the

crystal that do not rest on the mica, i.e. that are raised off the substrate, explaining the apparent increase in thickness.

Fig. 4 shows a low magnification image of a group of single crystals during the early stages of thickening at 90°C. Small thickened regions are indicated with arrows, and the dotted box shows the area imaged subsequently and shown in Figs. 5–7. In each of the images in Figs. 5 and 6 the bottom-right is the mica substrate while the rest of the image is the crystal in question. Figs. 5 and 6 show time sequences of part of the crystal shown in Fig. 4 during thickening. An arm of thickened material can be seen to “grow” down from the top left of the image towards the bottom. In this case the thickened material has a dendritic appearance. Fig. 6 shows a further sequence of images of the same area showing the progressive thickening of the crystal. A fairly regular front can be seen moving across the unthickened material. Occasionally holes open up at the front of the thickened region, temporarily halting the process until the thickening works its way around the edge of the hole. It is clear that the edge of the crystal had thickened first, before we started to image this crystal, causing some roughening of the originally crystallographic edge, although further thickening does not occur from this edge towards the centre of the crystal. From images such as these it is possible to measure the rate of growth of the thickened material, which was found to vary considerably from site to site, and over time in one area, but which was in the range 1–5 nm/s. In the final image in Fig. 6, taken after approximately 8 h of annealing at 90°C, it is apparent that the thickening process seems to have stopped, leaving a large expanse of apparently unthickened material. The heights of the thickened material, as measured by AFM, were in the range 14–17.5 nm. The upper part of this range is closely similar to the heights of extended chains tilted at 35° as explained above. The apparent discrepancy of some of these height measurements will be discussed below.

Fig. 7a shows a close up of part of the thickened structures, taken at the thickening temperature. Fig. 7b shows the area of the crystal imaged in Figs. 5 and 6 after cooling to room temperature. In this partially thickened crystal the heights correspond to tilted chains even after cooling to room temperature.

Fig. 8 shows a series of images of parts of two separate extended chain crystals of $C_{162}H_{326}$ during heating through the melting temperature. In successive images the points of the two crystals move towards each other until one has pushed up on top of the other, presumably due to thermal expansion of the crystal. In the final two images in the sequence the newly formed bi-layer has merged into a single layer and, particularly in the last image, the “crystal” has changed shape considerably. However, measurements of the cross-section still show a height corresponding to the (tilted) extended chains, and an edge profile that is as sharp as it was at lower temperatures (and probably corresponds to the profile of the imaging tip). Towards the top of the last scan the image quality deteriorated significantly until

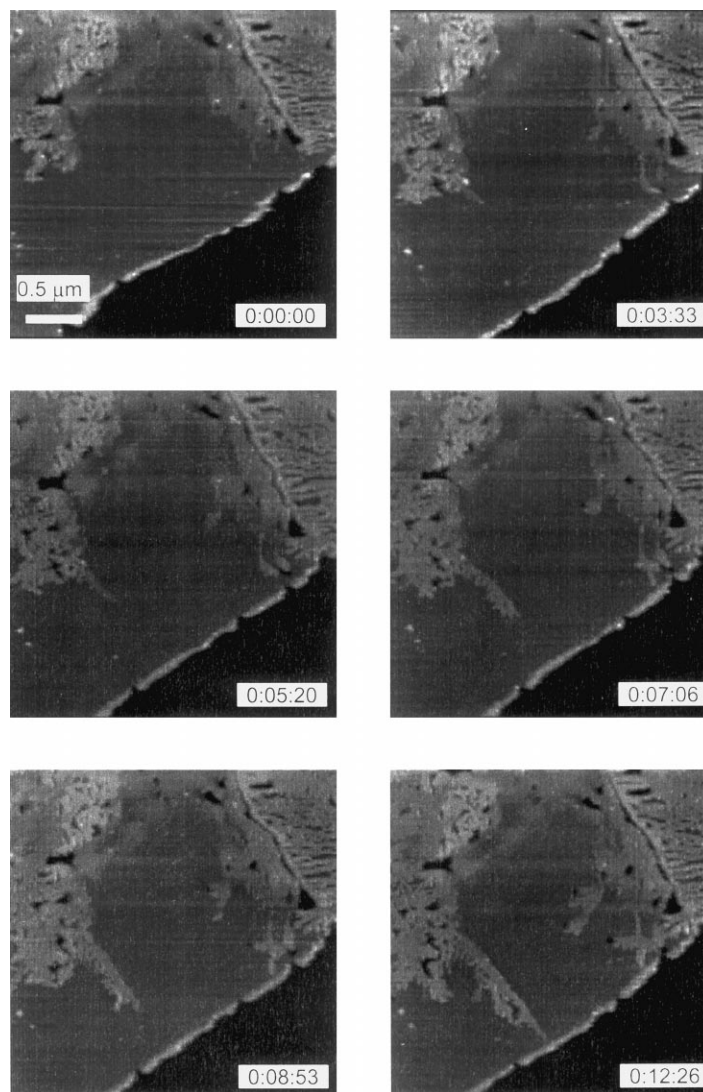


Fig. 5. The first series of height images obtained during the isothermal thickening of once-folded $C_{162}H_{326}$ at $90^{\circ}C$. Images were consecutively at a rate of one image every 85 s.

control was lost. On cooling immediately to room temperature it was found that the sample had melted, breaking up into droplets which crystallised to form spherulites at some point during the cooling process. From these images we can calibrate the temperature lag between the sample and the Linkam hot-stage as $11^{\circ}C$. In the previous experiments we would expect the temperature lag to be considerably less as there was no need for the nitrogen gas flowing over the heat shield (which protects the piezo tube from damage at higher temperatures). It is clear from these images that, apart from the slight drift of the two crystals towards each other, there is little change in shape of these extended chain crystals during heating or during imaging at these elevated temperatures, until just before melting. In particular, the surface of the crystal remains flat and no holes are formed. The edges of the crystals appear to become smoother as the sample is heated, which may be due to a pre-melting effect as the molecules begin to transform into a more mobile phase.

This experiment implies that the height calibration of the piezo scanner has not changed significantly at these elevated temperatures.

4. Discussion

Using the AFM we have been able to image the thickening of once-folded $C_{162}H_{326}$ crystals into the extended chain form, in real time, obtaining both kinetic and morphological information that has not previously been accessible. However, before discussing these results further, the first question that needs to be addressed is the extent to which we are interfering with the thickening process by observing it. In particular, whether the action of the tip on the surface is either acting to enhance thickening, or to create holes in the relatively soft crystals at these elevated temperatures. From studying the images presented here, and others like

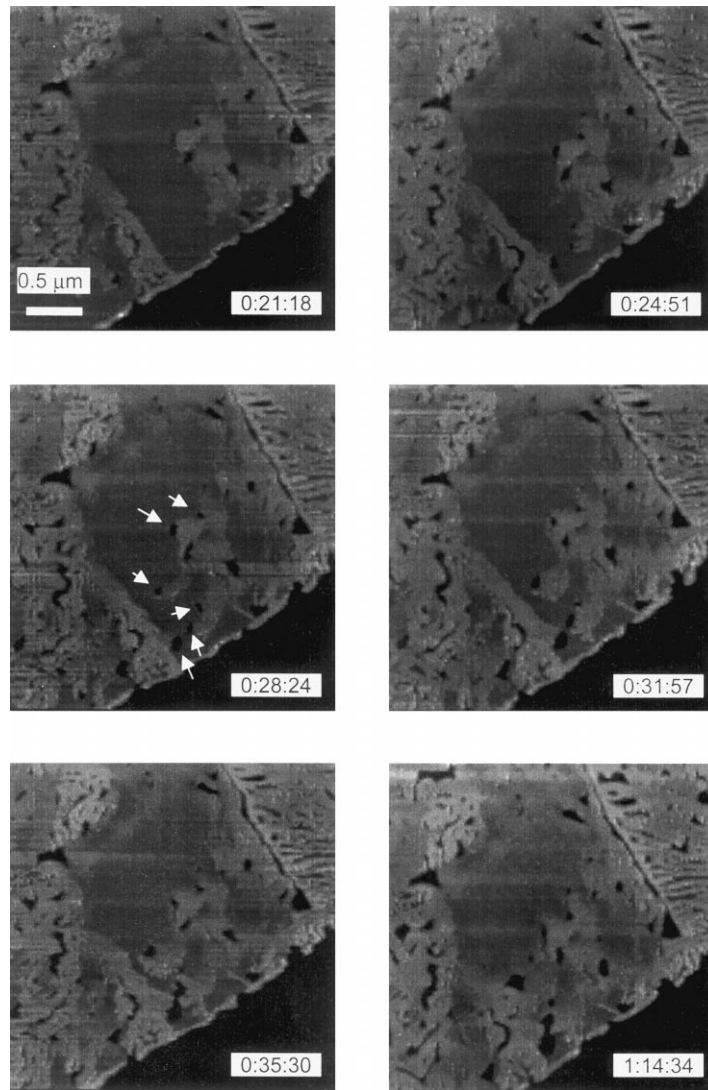


Fig. 6. The second series of height images for the annealing experiment carried out at 90°C. Towards the end of this sequence the process all but stops. Once again each image was acquired in 85 s. The arrows in the third image demonstrate the observation that the holes are often nucleated at the “growth front” of the extended phase.

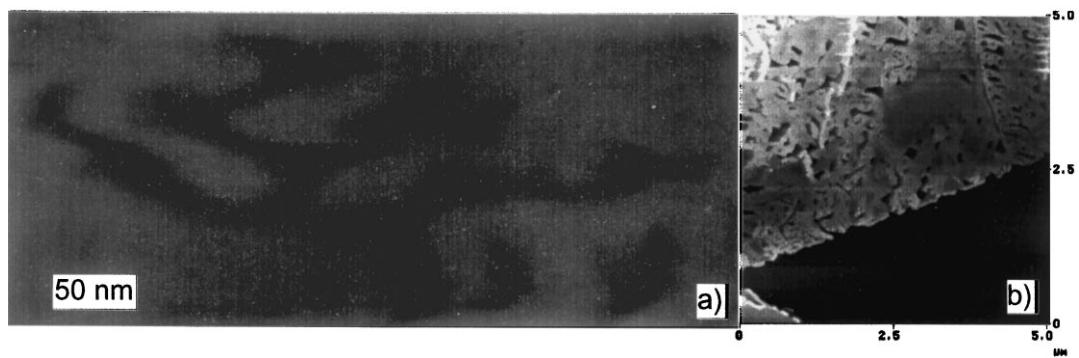


Fig. 7. (a) A higher resolution height image of an area near that of Figs. 5 and 6 shows a dendritic pattern in the depleted region; (b) An image taken at room temperature.

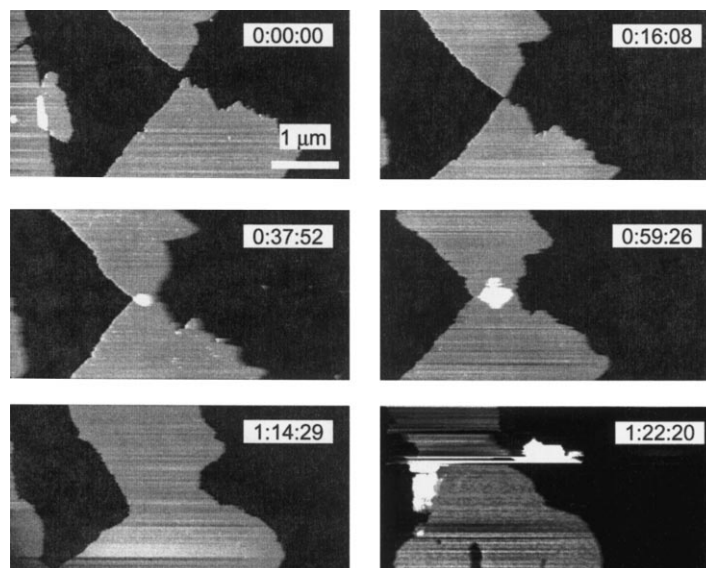


Fig. 8. A sequence of images of extended-chain $C_{162}H_{326}$ crystals being heated. The sequence starts at a nominal temperature of 101°C . It is heated at a rate of $0.4^{\circ}/\text{min}$ until it melts at a nominal temperature of 134°C . The acquisition time is approximately 130 s per image.

them, there is no evidence of preferential thickening in particular directions relative to the scan direction. Similarly, by comparing the areas that we have been imaging with both adjacent areas on the same crystal, and with other crystals, both after cooling to room temperature and at the thickening temperature, we have found no difference in the thickened morphologies—no influence of our observation of thickening is apparent. Finally, the extended chain crystals, which do not undergo thickening (as they are already in their equilibrium conformation), do not change during heating until just before they melt (and then not by forming holes), supporting our belief that the tip is not responsible for forming holes in the crystals as it images them. We are therefore able to state with some confidence that the data obtained are of the thickening process as it occurs at that temperature, and discuss it accordingly.

A second question that needs to be addressed before continuing further is that of the actual thicknesses measured. In particular, why the thickness after thickening was not always exactly equal to that of either a perpendicular or tilted extended chain, and frequently appeared somewhat thinner than we might expect. It may be that, as we were scanning relatively quickly, there was some thinning due to the scan speed, as has been reported elsewhere [31]. However, the scan speeds used in our experiments were not as fast as those suggested to give considerable thinning. An alternative explanation is that there was a fine scale structure of thickened and unthickened regions that was not resolved by the tip and which leads to a height averaging taking place in each pixel between the height of the extended and once-folded material. There are indications from some areas of the images shown that such a fine scale structure was in fact present (and, given the drift and lack of stability at these elevated temperatures, may not be

resolvable using the standard AFM tips). Finally, it may be that at these high temperatures the material is sufficiently soft (especially at the edges of the thickened regions) that there is some depression in the measured height as the probe penetrates slightly into the crystal surface. All of these explanations may play a part in the slight depression in the measured heights. However, in most areas, especially those where there were large expanses of thickened material, the heights measured were closely similar to those expected for extended chains with a 35° tilt to the lamellar normal.

The first observation that can be made, regarding the thickening process itself, is that it is one of nucleation and growth—thickening started at some site or sites within the relatively large crystal, outside the area that was being imaged, and spread across the rest of the crystal. Nucleation events are clearly relatively rare, as there was no further nucleation within the area that we were imaging during the 8 h of the isothermal experiment. A secondary process, particularly apparent in Fig. 2, is the preferential thickening of the edges of the crystal, presumably as the molecules along the edge have a higher level of mobility due to the limited extent of the lattice in which they reside, although surprisingly these thickened edges do not lead to subsequent thickening towards the middle of the crystal.

In the two separate experiments reported here somewhat different morphologies developed. In particular, after cooling to room temperature the morphology developed after annealing at $\sim 110^{\circ}\text{C}$ and thickening during heating, resembles the morphologies commonly seen after thickening high polymers on a substrate—the “Swiss cheese” morphology. In contrast, the lower temperature, isothermal annealing experiment gave a more complex structure, in which unthickened material remained after long annealing times,

and where the thickened material had a fine scale roughness not seen after annealing at higher temperatures. We believe that this is due to the high level of chain mobility that existed at the higher temperatures, in which material could migrate along the rough surface of the holes formed by the thickening process, allowing any unthickened material to unfold. Indeed, we have preliminary indications that such a high level of mobility does exist at these elevated temperatures, a subject which is currently receiving attention in our laboratory.

The thickening morphology followed in the isothermal thickening experiment (Figs. 4–7), is of considerable interest. In many cases fingers of thickened material grow into the unthickened matrix, often with a point no more than 20 nm in diameter. Side branches then grow off this finger which, at the same time, widens. This mode of growth is commonly seen in diffusion limited processes [32], in which growth (or in our case conversion from 1F to extended chain crystal) occurs most rapidly by fine tips that are able to penetrate through a depletion layer that builds up ahead of the growth front. In our case it seems most likely that the necessary strain caused in the lattice by the reduction in top-surface area, while volume is conserved in these isolated layers, is limiting the thickening process. This strain needs to “diffuse” away from the thickening front, and causes the dendritic structure, in a similar manner to that postulated by one of us in solution thickening of alkanes [4]. The formation of dendritic patterns is common in polymeric materials; a recent example of such patterns in absorbed polymer monolayers being that by Reiter and Sommer [33]. In some cases unthickened material is then trapped between the thickened fingers of material, as shown in Fig. 7a. Here it may be that there is a competition between the reduction in free energy that thickening allows, with the increase in free energy necessary to create the large additional surface of the hole, resulting in the unthickened material being stabilised in a state of quasi-equilibrium.

In some areas a somewhat different mode of thickening occurs in which a large front of thickened material grows across the unthickened matrix. In this case holes frequently open up at the thickening front, arrowed in Fig. 6f. Here, instead of the lattice strain (or possibly chain vacancies) being bypassed by the thickening front, they build up until eventually sufficient strain is present to nucleate a hole. This hole then has to be bypassed by the thickening front in order for more material to be converted, and acts to temporarily halt the thickening process. In many instances a combination of the above processes is seen, with holes opening in front of dendritic fingers.

Why there should be these apparently different modes of thickening is unclear. It may be that the original composition of the crystal, and in particular its degree of perfection, varies. Slightly higher than average defect levels might lead

to preferential thickening in certain areas, encouraging the formation of dendritic structures.

Another question that arises is the extent to which both the underlying crystallography, and the direction of folding, influence the thickening process. The crystal that has been imaged here during isothermal thickening is a rectangular 110 twin. The 110 fold planes will lie at an angle of $\sim 67^\circ$ to the edge of the crystal, although, as we did not image the re-entrant corner of the crystal, the actual direction (i.e. to the left or to the right of the image) is unknown. The 100 and 010 planes, along which preferential thickening is sometimes seen, lie at an angle of ~ 56 and $\sim 34^\circ$ to the edge of the crystal in our images. From our data the only preferential directions of thickening appear to be perpendicular, and perhaps parallel, to the edge of the crystal, which is somewhat surprising and in contradiction to the observations on isothermal thickening in solution. Similarly the holes themselves give little indication of the underlying crystallography. In the work presented here we have chosen an annealing temperature so as to minimise the rate at which thickening occurs. The degree of molecular mobility, and the rate of solid state diffusion, is most likely very low at these temperatures. Also, as thickening is occurring between once-folded and extended chain growth, the extent to which the direction of folding influences the rates of molecular transport will be considerably reduced when compared to molecules containing more folds. These factors may all act so as to suppress the influence of the crystallography on the thickening process.

The main subject of this paper is the isothermal thickening behaviour of 1F $C_{162}H_{326}$ into the extended form. However, an additional experiment in order to assess whether the act of imaging the surface was creating holes, has also been reported here, in which as crystallised, extended chain crystals were imaged during heating and melting. This experiment, while helping to confirm that we were not substantially influencing the thickening process, also proved surprising in that a high level of mobility, as evidenced by large scale changes in crystal shape, occurred just before melting. From measurements of thickness it appears that the chains were at least still oriented at approximately the 35° tilt angle present in the previous images (giving a thickness ~ 17 nm although the level of surface roughness had increased substantially) and the edges of the “crystal” are still sharp. It seems unlikely that the thickness would be maintained after melting unless dewetting was a considerable problem, which it clearly is not, as the shape of the “crystal” has changed considerably. Therefore the chains must still be straight and aligned, but very mobile. Whether this is a mobile, rotator type phase is unclear. It seems likely that such a phase would be stabilised by the unique constraint placed on the system by melting a single layer on a substrate—the co-operative motion required for melting is constrained largely to two dimensions. Further work in this area is clearly required.

5. Conclusions

Using atomic force microscopy we have been able to image the thickening of single crystals of $C_{162}H_{326}$ from the once-folded to the extended form, in situ, in real time. Consecutive images have been obtained allowing the kinetics of thickening to be followed on a scale of tens of nanometres, and the development of thickened morphologies to be imaged directly, in a manner that has not been possible using other techniques.

The formation of dendritic structures has been followed and we have postulated that these are caused by the necessity for strain in the lattice to diffuse away from the thickening front. Holes have been found to nucleate primarily at the thickening front, relieving the strain in the lattice but at the same time changing the direction of the thickening front.

Extended chain crystals have been found to melt without the formation of holes, although a highly mobile phase is entered just before true melting occurs. Whether this mobile phase is due solely to the stabilising influence of the substrate is, at this stage, unknown.

The power of high temperature atomic force microscopy, coupled with high purity, monodisperse materials, to improve our understanding of dynamic processes such as polymer crystal thickening, is clear.

Acknowledgements

We would like to thank G. Brooke for the synthesis of the materials. AKW and JKH would like to thank the EPSRC for funding. The authors would like to acknowledge the contribution of the late Andrew Keller to this work. Before his death we had, amongst much else, discussed the possibilities of using AFM for studying thickening in the alkanes. His knowledge and passion were an inspiration to us all.

References

- [1] Organ SJ, Barham PJ, Hill MJ, Keller A, Morgan RL. *J Polym Sci PartB: Polym Phys Ed* 1997;35:1775.
- [2] Morgan RL, Barham PJ, Hill MJ, Keller A, Organ SJ. *J Macromol Sci—Phys* 1998;37:319.
- [3] Hobbs JK, Hill MK, Keller A, Barham PJ. *J Polym Sci PartB: Polym Phys Ed* 1999;37:3188.
- [4] Hobbs JK, Hill MJ, Barham PJ. Submitted for publication.
- [5] Brooke GM, Burnett S, Mohammed S, Proctor D, Whiting MC. *J Chem Soc Perkin Trans 1* 1996:13.
- [6] Ungar G, Steyny J, Keller A, Bidd I, Whiting MC. *Science* 1985;229:386.
- [7] Ungar G, Keller A. *Polymer* 1987;28:1899.
- [8] Ungar G, Keller A. *Polymer* 1986;27:1835.
- [9] Organ SJ, Ungar G, Keller A. *J Polym Sci PartB: Polym Phys Ed* 1990;28:2365.
- [10] Ungar G, Organ SJ. *J Polym Sci PartB: Polym Phys Ed* 1990;28:2353.
- [11] Zeng XB, Ungar G. *Polymer* 1998;39(19):4523.
- [12] Keller A, O'Connor A. *Discuss Faraday Soc* 1958;25:114.
- [13] Wunderlich B. *Crystal nucleation, growth, annealing, Macromolecular physics*, 2. New York: Academic Press, 1976 (chap. 7).
- [14] Geil PH. *Polymer single crystals, Polymer reviews*. New York: Wiley, 1963 (chap. 5).
- [15] Dlugosz J, Fraser GV, Grubb D, Keller A, Odell JA, Goggin PL. *Polymer* 1976;17:471.
- [16] Rastogi AB, Spoelstra JGP, Goossens PJ, Lemstra. *Macromolecules* 1997;30(25):7880.
- [17] Organ SJ, Keller A. *J Mater Sci* 1985;20:1586.
- [18] Dreyfuss P, Keller A. *J Macromol Sci—Phys* 1970;B4(4):811.
- [19] Binnig G, Quate CF, Gerber Ch. *Phys Rev Lett* 1986;56(9):930–3.
- [20] Binnig G, Rohrer H, Gerber Ch, Weibel E. *Appl Phys Lett* 1982;40:178–80.
- [21] Drake B, Prater CB, Weisenhorn AL, Gould SAC, Albrecht TR, Quate CF, Cannell DS, Hansma HG, Hansma PK. *Science* 1989;243(4898):1586–9.
- [22] Pearce R, Vancso GJ. *Polymer* 1998;39(5):1237–42.
- [23] Schultz JM, Miles MJ. *J Polym Sci PartB: Polym Phys Ed* 1998;36(13):2311–25.
- [24] Hobbs JK, McMaster TJ, Miles MJ, Barham PJ. *Polymer* 1998;39(12):2437–46.
- [25] McMaster TJ, Hobbs JK, Barham PJ, Miles MJ. *Probe Microsc* 1997;1:43.
- [26] Ivanov DA, Nysten B, Jonas AM. *Polymer* 1999;40(21):5899–905.
- [27] Sakai Y, Imai M, Kaji K, Tsuji M. *J Crystal Growth* 1999;203(1–2):244–54.
- [28] Chen X, Shakesheff KM, Davies MC, Heller J, Roberts CJ, Tendler SJB, Williams PM. *J Phys Chem* 1995;99(29):11537–42.
- [29] Iwata T, Doi Y, Tanaka T, Akehata T, Shiromo M, Teramachi S. *Macromolecules* 1997;30(18):5290–6.
- [30] Thomson NH, Miles MJ, Ring SG, Shewry PR, Tatham AS. *J Vac Sci Technol B* 1994;12(3):1565–8.
- [31] Hanley SJ, Giasson J, Revol J-F, Gray DG. *Polymer* 1992;33(21):4639.
- [32] Glicksman ME, Marsh S. In: Hurler DTJ, editor. *Fundamentals: transport and stability, Handbook of crystal growth*, 1b. Amsterdam: North-Holland, 1993 (chap. 15).
- [33] Reiter G, Sommer JU. *Phys Rev Lett* 1998;80(17):3771–4.